

Comp Astro Assignment 1

Cameron Smith

March 31, 2021

Part 1

While the fourth order Runge-Kutta method gives a good approximation of the ODE, it has no built-in way of conserving necessary quantities such as angular momentum or energy. This results in orbits such as the one in Figure 1(f), where the particle gets closer and closer to the mass at the origin, speeding up as it goes, until it's finally ejected altogether. This lack of conservation means that the errors can build up, with both the angular momentum and total energy of the system decreasing over time, causing the orbit to decay (see Figures 2(d) and 2(b)). On the other hand, while the leapfrog scheme is only second order, it is able to conserve angular momentum and the error in the total energy is symmetric and does not increase over time, as can be seen in Figures 2(a) and 2(c). As a result, the orbit does not decay over time, however does rotate if the timestep is too large, as can be seen in Figures 1(c) and 1(e).

Part 2

a)

Figure 3 shows the “1.75D” magnetised shock at $t = 0.2$. The red and blue discontinuities correspond to fast and slow waves respectively, corresponding to the two solutions in the dispersion relation for compressive waves ($\mathbf{v} \cdot \mathbf{k} \neq 0$). Because they are compressive waves, they are present in every plot. The speed of these waves is given by:

$$v_{wave}^2 = \frac{\omega^2}{k^2} \quad (1)$$

$$= \frac{1}{2} \left[c_s^2 + v_A^2 \pm \sqrt{(c_s^2 + v_A^2)^2 - 4c_s^2 v_A^2 \cos^2 \theta} \right], \quad (2)$$

But we have

$$\cos \theta = \hat{\mathbf{k}} \cdot \frac{\mathbf{B}_0}{|B_0|} \quad (3)$$

$$c_s^2 = \frac{\gamma P^2}{\rho^2}, \text{ and} \quad (4)$$

$$v_A^2 = \sqrt{B_0^2 / (\mu_0 \rho_0)}. \quad (5)$$

For $x < 0$, and therefore waves travelling to the left, we have:

$$\rho_0 = 1.08, \quad (6)$$

$$P_0 = 0.95, \quad (7)$$

$$\mathbf{B}_0 = (2/\sqrt{4\pi}, 3.6/\sqrt{4\pi}, 2/\sqrt{4\pi})^T, \text{ and} \quad (8)$$

$$\hat{\mathbf{k}} = (-1, 0, 0)^T \quad (9)$$

$$\gamma \approx 1.7 \quad (10)$$

This gives

$$v_{wave} = 0.39, \quad (11)$$

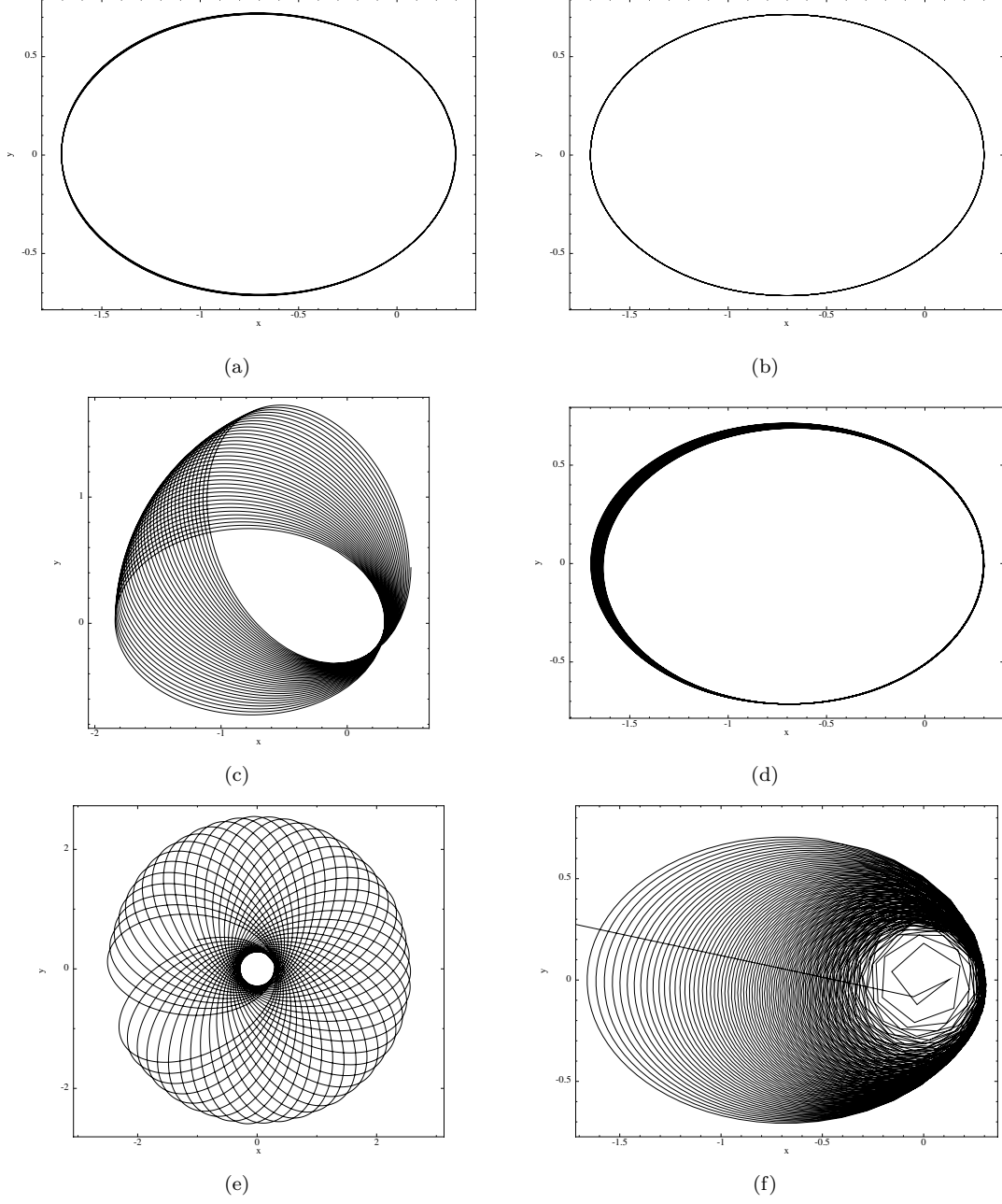


Figure 1: Calculated orbits using the second order Leapfrog/Velocity Verlet scheme (left) and the fourth order Runge-Kutta method (right), using time steps of 0.01 (top) 0.05 (middle) and 0.1 (bottom).

for the slow wave (taking the minus), and

$$v_{wave} = 1.7, \quad (12)$$

for the fast wave. Similarly, For $x > 0$ (waves travelling to the right), we have:

$$\rho_0 = 1, \quad (13)$$

$$P_0 = 1, \quad (14)$$

$$\mathbf{B}_0 = (2/\sqrt{4\pi}, 4/\sqrt{4\pi}, 2/\sqrt{4\pi})^T, \text{ and} \quad (15)$$

$$\hat{\mathbf{k}} = (1, 0, 0)^T \quad (16)$$

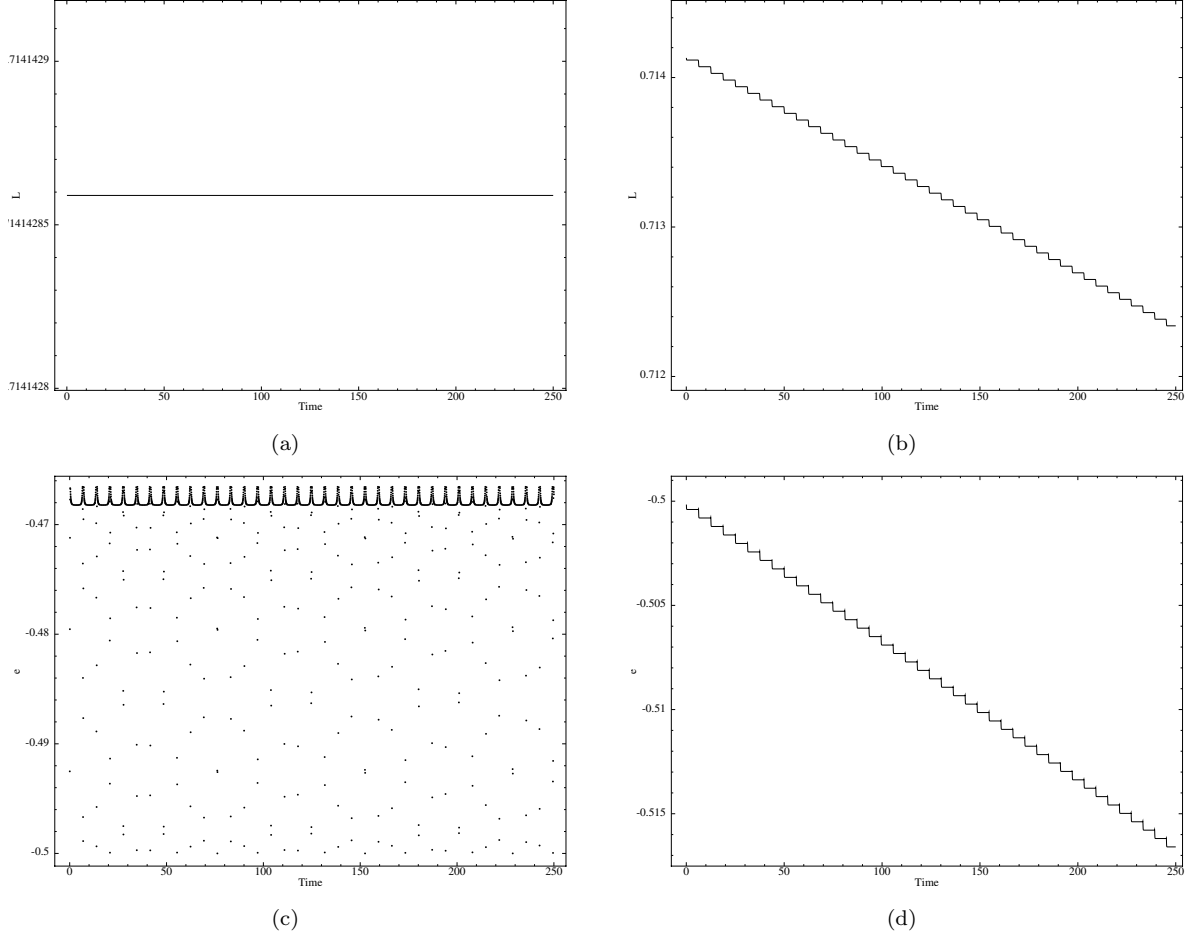


Figure 2: Angular momentum (top) and total energy (bottom) versus time of the orbits using the second order Leapfrog/Velocity Verlet scheme (left) and the forth order Runge-Kutta method (right).

This gives

$$v_{wave} = 0.39, \quad (17)$$

for the slow wave (taking the minus), and

$$v_{wave} = 1.8, \quad (18)$$

for the fast wave.

$$(19)$$

The Alfvén waves are not compressive, but can be seen in the plots of the magnetic field and, as well as the velocity in the x and y directions (see Figure 3). The speed of the Alfvén waves can be found from the dispersion relation as follows:

$$v_{wave}^2 = \frac{\omega^2}{k^2} \quad (20)$$

$$= v_A^2 \cos^2 \theta, \quad (21)$$

For $x < 0$, this gives

$$v_{wave} = 0.54, \quad (22)$$

while for $x > 0$ this gives

$$v_{wave} = 0.56. \quad (23)$$

Therefore the speed of the Alfvén waves is in between the speed of the slow and fast waves. This is also reflected on the plots in Figure 3.

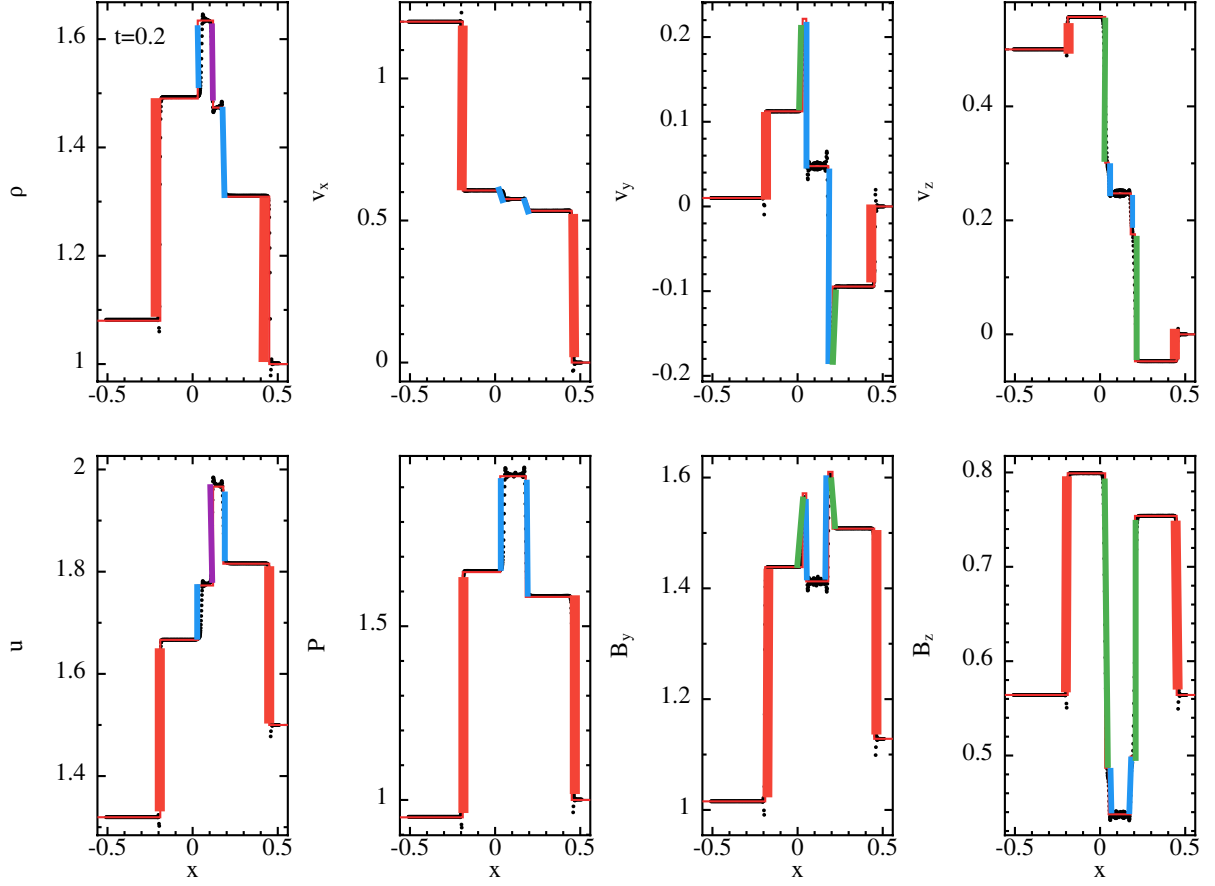


Figure 3: The “1.75D” magnetised shock tube. Red Corresponds to a fast wave, blue corresponds to a slow wave, green corresponds to an Alfvén wave, and purple corresponds to a contact discontinuity.

b)

The initial Alfvén speed is given by:

$$v_A = \sqrt{B_0^2 / (\mu_0 \rho_0)}. \quad (24)$$

We have:

$$b_0 = \frac{5}{\sqrt{4\pi}}, \quad (25)$$

$$\mu_0 = 1, \text{ and} \quad (26)$$

$$\rho_0 = 1, \quad (27)$$

giving:

$$v_A \approx 1.4. \quad (28)$$

Similarly, since $\gamma = 1.4$ and $P_0 = 1$ (see Figure 4), we find:

$$c_s = \sqrt{\frac{\gamma P_0}{\rho_0}} \quad (29)$$

$$\approx 1.18 \quad (30)$$

For waves traveling in the x direction ($\cos \theta = 1$), Equation 2 reduces to

$$v_{wave} = c_s \quad (31)$$

for slow waves, and

$$v_{wave} = v_A \quad (32)$$

for fast waves. In the case of Alfvén waves, Equation 21 reduces to

$$v_{wave} = v_A. \quad (33)$$

Similarly, for waves travelling in the y direction ($\cos \theta = 0$), we get velocities of $v_{wave} = 0$ for slow and Alfvén waves, and $v_{wave} = \sqrt{c_s^2 + v_A^2} \approx 1.84$ for fast waves. Using the approximation:

$$x = x_0 + v_{wave}t, \quad (34)$$

we find that at $t = 0.15$, the slow, fast and Alfvén waves reach distances of $x = 0.28, 0.31, 0.31$ and $y = 0.1, 0.38, 0.1$ respectively.

We note that the fast waves travel in both the x and y direction, and are slightly faster in the y direction. These are compressive waves, and should be visible in all the plots. Meanwhile, the slow waves travel mainly in the x direction (they do not travel in the y direction), and should also be visible in all plots as they are also compressive. The Alfvén waves mainly travel in the x direction (the direction of the magnetic field), and should be visible in the plot of the magnetic energy. Importantly, these waves are not compressive, and so should not show up in either the pressure or density plots. We therefore label the shockfronts as shown in Figure 4.

Part 3

a)

The gas and dust velocities after 5 wave periods are show in Figure 5(a) for the one fluid method, and Figure 5(b) for the two fluid method.

b)

See end of document.

c)

The stopping time is given by

$$t_s = \frac{\rho_g \rho_d}{K(\rho_g + \rho_d)}. \quad (35)$$

In our case we have $\rho_g = \rho_d = 1$, and so we find

$$t_s = \frac{1}{2K}. \quad (36)$$

We have values of $K = 0.001, 0.01, 1.0, 100, 1000$, which give stopping times of $t_s = 500, 50, 0.5, 0.005, 0.0005$ respectively. For small K , (large stopping time), the dispersion relation reduces to

$$\omega^2 = k^2 c_s^2, \quad (37)$$

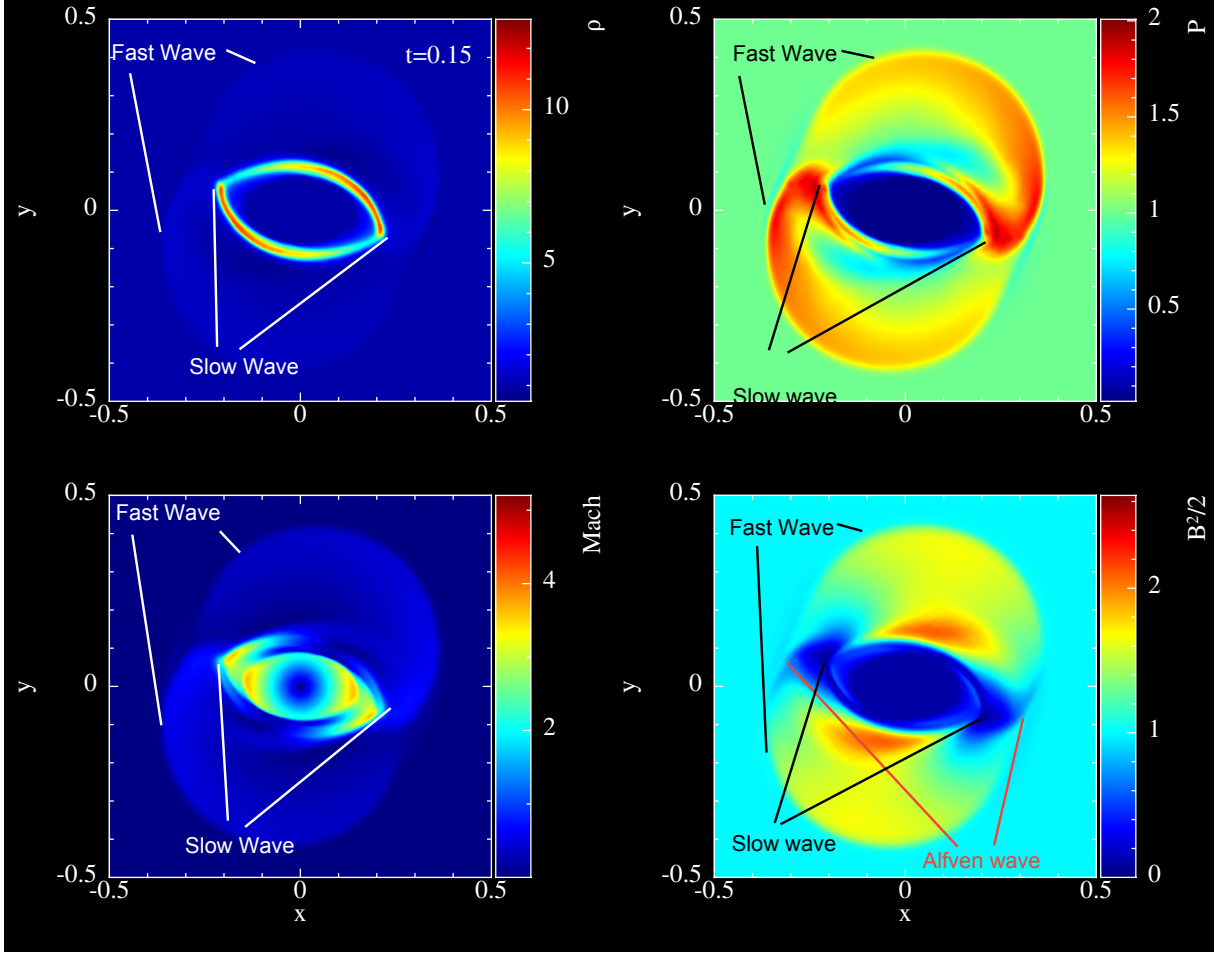


Figure 4: The 2D MHD rotor test, showing the density (ρ), pressure (P), mach number (Mach), and magnetic energy ($B^2/2$). The shockfronts for the fast waves, slow waves and Alfvén waves are labeled.

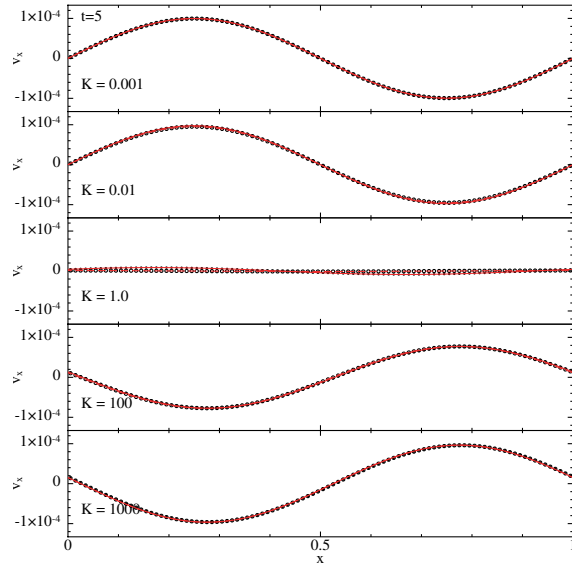
while for large K , (small stopping time), the dispersion relation reduces to

$$\omega^2 = k^2 \tilde{c}_s^2. \quad (38)$$

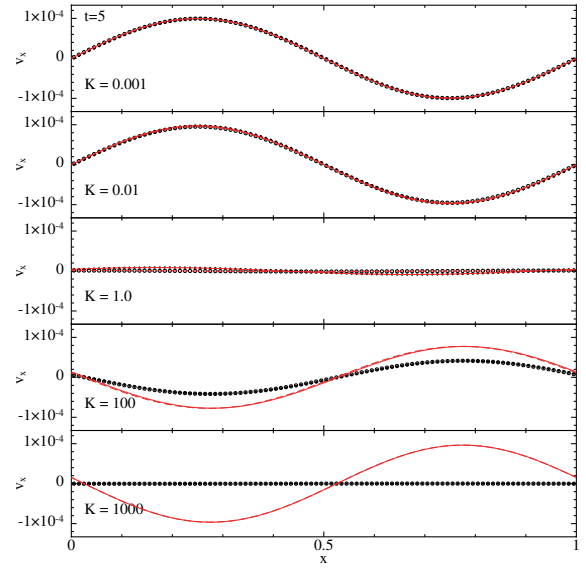
In either case, there is no (or negligible) dampening term, and so the wave remains undamped, as can be seen in Figures 5(a) and 5(b) for both large and small K . The only case where dampening comes into effect is when $t_s \omega \sim 1$, i.e. the stopping time is similar to the timescales involved. This can be seen for the $K = 1.0$ case these figures.

d)

The two fluid method gives accurate results for small K (i.e. large stopping times), which occurs when the two fluids are weakly coupled. Assuming Epstein drag, this corresponds to large grains. As we are dealing with only (small) linear perturbations, the one fluid method is able to approximate the analytic solution for all values of K shown in figure 5(a). However unlike the two fluid method, for small K this can break down for non linear perturbations as it is unable to handle double valued solutions (i.e. dust particles passing through each other). Typically the one fluid method gives the most accurate results for large K (small stopping times), when the two fluids are strongly coupled. This corresponds to small grains.



(a)



(b)

Figure 5: The dusty wave problem for a variety of K values using the one fluid method (a) and the two fluid method (b).